ACS APPLIED MATERIALS & INTERFACES

Research Article

www.acsami.org

Cosensitization of D-A-π-A Quinoxaline Organic Dye: Efficiently Filling the Absorption Valley with High Photovoltaic Efficiency

Kai Pei,[†,§] Yongzhen Wu,[†,§] Hui Li,[†] Zhiyuan Geng,[‡] He Tian,[†] and Wei-Hong Zhu*[,†]

[†]Shanghai Key Laboratory of Functional Materials Chemistry, Key Laboratory for Advanced Materials and Institute of Fine Chemicals, Collaborative Innovation Center for Coal Based Energy (i-CCE), East China University of Science and Technology, Shanghai 200237, P. R. China

[‡]Gansu Key Laboratory of Polymer Materials, College of Chemistry and Chemical Engineering, Key Laboratory of Eco-environment-related Polymer Materials, Ministry of Education, Northwest Normal University, Lanzhou, 730070 Gansu P. R. China

Supporting Information

ABSTRACT: In the efficient cosensitization, the pure organic sensitizers with high molecular extinction coefficients and long wavelength response are highly preferable since the dye loading amount for each dye in cosensitization is decreased with respect to single dye sensitization. A D-A-π-A featured quinoxaline organic sensitizer **IQ21** is specifically designed. The high conjugation building block of 4*H*-cyclopenta[2,1-*b*:3,4-*b*′]dithiophene (CPDT) is introduced as the π bridge, instead of the traditional thiophene unit, especially in realizing high molecular extinction coefficients (up to 66 600 M^{-1} cm^{-1}) and extending the light response wavelength. With respect to the reference dye **IQ4**, the slightly lower efficiency of **IQ21** (9.03%) arises from the decrease of V_{OC}, which offsets the gain in J_{SC}. While cosensitized with a smaller D-π-A dye **S2**, the efficiency in **IQ21** is further improved to 10.41% (J_{SC} = 19.8 mA cm^{-2}, V_{OC} = 731 mV, FF = 0.72). The large improvement in efficiency is attributed to the well-matched molecular structures and loading amounts of both dyes in the cosensitization system. We also demonstrated that coabsorbent dye **S2** can distinctly compensate the inherent drawbacks of **IQ21**, not only enhancing the response intensity of IPCE, making up the absorption defects around low wavelength region of IPCE, but also repressing the charge recombination rate to some extent.

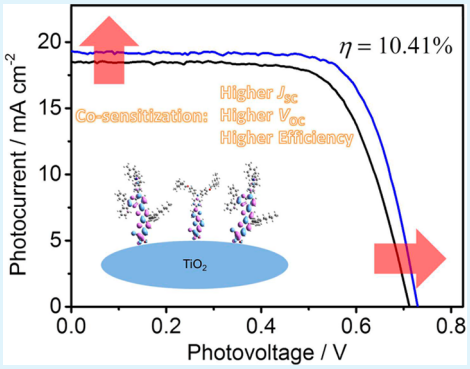

KEYWORDS: *dye sensitized solar cells, cosensitization, quinoxaline, π-bridges, photovoltaic efficiency*

INTRODUCTION

The increasing demand for clean and renewable energy has aroused great enthusiasm for solar energy conversion in a global scale. In dye-sensitized solar cells (DSSCs),[1,2] the donor-π bridge-acceptor (D-π-A) model has been well-recognized as constructing high-performance organic sensitizers.[3−9] Its specific intramolecular charge transfer (ICT) band is extremely helpful to harvest sun light and thus to generate photocurrent in solar cells. However, the ICT absorption band in most organic sensitizers is not broad enough to efficiently cover the solar photon-flux spectrum, alone with an unpreferable incident photon-to-current conversion efficiency (IPCE). Except ruthenium complexes and porphyrin-based dyes, the photovoltaic efficiency for the majority of metal-free pure organic sensitizers always falls in the range of 3−9%.[10−14] Indeed, the efficiency greater than 10% based on pure organic sensitizers is rarely achieved, especially with traditional iodine electrolyte.[15−19]

In this respect, the cosensitization based on multiple dyes as "dye cocktails"[20−26] has been exploited, especially in compensating and broadening the light response region.[27,28] In the specific cocktail cosensitization, two or more kinds of dyes with complementary absorption spectra are coadsorbed onto the TiO_2 photoanode. Generally, the cosensitization strategy needs well-understood intermolecular interactions between or among the coadsorbed dyes, especially with the matchable size, shape, and orientations as well as compensating light-harvest. Also we have to delicately optimize the loading ratio or time of coadsorbed dyes. For the efficient cosensitization, the pure organic sensitizers with high molecular extinction coefficients and long wavelength response are highly preferable since the dye loading amount for each dye in cosensitization is decreased with respect to single dye sensitization. Until now, except for ruthenium complexes[27] or porphyrin dyes,[29−31] the strategy with cosensitization approach has often been quite unsuccessful so far in conjunction with pure organic sensitizers.

Herein we focus on the absorption capability and response wavelength of pure organic dyes and employ a cosensitization strategy to the quinoxaline-based dye **IQ21** (Figure 1) for

Received: December 7, 2014
Accepted: February 24, 2015
Published: February 24, 2015

DOI: 10.1021/am508623e
ACS Appl. Mater. Interfaces 2015, 7, 5296−5304

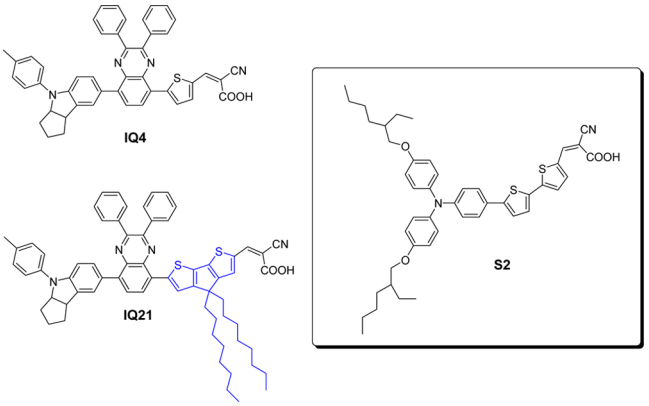

Figure 1. Chemical structures of sensitizer **IQ21**, cosensitizer **S2**, and reference dye **IQ4**.

enhancement in photovoltaic efficiency. On the basis of the rational molecular design, the high conjugation building block of 4*H*-cyclopenta[2,1-*b*:3,4-*b*′]dithiophene (CPDT)[32−35] is introduced as the π bridge, instead of the traditional thiophene unit, especially in realizing high molecular extinction coefficients (up to 66 600 M^{-1} cm^{-1}, 2.60-fold greater than that of the reference dye **IQ4**[36] and extending the light response wavelength. Moreover, a D-π-A featured dye **S2**[28] is screened as coadsorbent dye for efficiently filling the absorption valley of **IQ21** in the range of at 300−470 nm. Because of the distinct increase in molar coefficient and the matchable absorption in light harvesting, the delicate cosensitization with **IQ21** and **S2** realizes a promising high efficiency of 10.41% under AM 1.5G illumination at 100 mW cm^{-2}. We provide a clear method how to rationally increase molecular extinction coefficients, and step by step optimize photovoltaic efficiency with cocktail cosensitization, along with exploring cosensitized dye with matchable molecular size, shape, and orientations.

EXPERIMENTAL SECTION

Characterization. ^1H and ^{13}C NMR spectra were recorded on Bruker AVANCE III-400 MHz (100 MHz for ^{13}C NMR) instruments with tetramethylsilane as internal standard. High-resolution mass spectrometry (HRMS) was performed using a Waters LCT Premier XE spectrometer. The absorption spectra of sensitizer dyes in solution and adsorbed on TiO_2 films were measured with a Varian Cary 500 spectrophotometer. The cyclic voltammograms (CV) were determined with a Versastat II electrochemical workstation (Princeton Applied Research) using a three-electrode cell with a Pt working electrode, a Pt wire auxiliary electrode, and a saturated calomel (SCE) reference electrode in saturated KCl solution, and 0.1 M tetrabutylammonium hexafluorophosphate ($TBAPF_6$) was used as the supporting electrolyte in CH_2Cl_2. Ferrocene was added to each sample solution at the end of the experiments, and the ferrocenium/ferrocene (Fc/Fc^+) redox couple was used as an internal potential reference.

Synthesis. The synthetic route is depicted in Scheme S1 in Supporting Information. **IQ21** was synthesized from the starting material of 5,8-dibromo-2,3-diphenylquinoxaline and obtained in a moderate yield via common Suzuki coupling and Vilsmeier−Haack and Knoevenagel condensation reactions.

Synthesis of IQ21. A mixture of aldehyde **21c** (150 mg, 0.16 mmol) and cyanoacetic acid (17 mg, 0.20 mmol) in acetonitrile (16 mL) was refluxed in the presence of piperidine (0.5 mL) for 7 h under argon. After it cooled, the mixture was diluted with CH_2Cl_2, washed with water and brine, dried over Na_2SO_4, and evaporated under reduced pressure. The crude product was purified by column chromatography with 1% acetic acid in CH_2Cl_2 on silica gel to yield the product as a purple powder (100 mg, 0.10 mmol, yield 63%). ^1H NMR (400 MHz, deuterated tetrahydrofuran (THF-d_8,) ppm): δ 8.24 (d, J = 8.8 Hz, 2 H), 7.90 (s, 1 H, thienyl-H), 7.77 (d, J = 8.0 Hz, phenyl-H), 7.63−7.73 (m, 4 H, phenyl-H), 7.51−7.58 (m, 3 H, phenyl-H), 7.43 (d, J = 8.0 Hz, phenyl-H), 7.27−7.36 (m, 3 H, phenyl-H), 7.10−7.24 (m, 4 H, phenyl-H), 7.04 (d, J = 8.4 Hz, phenyl-H), 6.89 (d, J = 8.0 Hz, phenyl-H), 4.73−4.83 (m, 1 H, indoline-CH−), 3.76−3.86 (m, 1 H, indoline-CH−), 2.20 (s, 3 H, indoline-CH_3), 1.99−2.10 (m, 1 H, indoline-CH_2−), 1.87−1.99 (m, 5 H, indoline-CH_2− and thienyl-C***H***$_2C_7H_{15}$), 1.79−1.86 (m, 1 H, indoline-CH_2−), 1.69−1.79 (m, 1 H, indoline-CH_2−), 1.41−1.55 (m, 2 H, indoline-CH_2−), 1.03−1.22 (m, 20 H, thienyl-CH_2C_5***H***$_{10}C_2H_7$), 0.86−1.02 (m, 4 H, thienyl-$C_6H_{12}C$***H***$_2CH_3$), 0.64−0.75 (m, 6 H, thienyl-$C_7H_{14}C$***H***$_3$). ^{13}C NMR (100 MHz, THF-d_8, ppm): δ 161.95, 158.15, 151.36, 151.13, 149.27, 147.72, 146.44, 145.01, 140.52, 139.83, 139.30, 130.25, 138.90, 138.64, 137.00, 136.76, 134.31, 130.89, 130.34, 130.07, 129.85, 129.49, 128.87, 128.55, 128.45, 128.18, 128.14, 127.81, 127.70, 127.00, 120.36, 119.79, 116.47, 106.81, 69.06, 53.64, 45.51, 37.80, 35.07, 33.65, 31.81, 30.06, 29.29, 22.52, 19.01, 13.45. IR (KBr-pellet, cm^{-1}): 3421.4, 3028.9, 2925.6, 2854.1, 1716.1, 1682.9, 1604.3, 1565.5, 1513.6, 1490.6, 1378.0, 805.6, 695.5. HRMS (ESI, m/z): $[M + H]^+$ calcd for $C_{67}H_{69}N_4O_2S_2$ 1025.4862, found 1025.4873.

Dye-Sensitized Solar Cell Fabrication and Photovoltaic Performance Measurements. A double-layer TiO_2 photoelectrode 17 μm in thickness, composed of a 12 μm thick nanoporous layer (DYSOL 18NR-T) and a 5 μm thick scattering layer (area: 0.12 cm^2), was prepared by screen printing on conducting glass substrate. The TiO_2 electrodes were gradually heated under an air flow at 275 °C for 5 min, at 325 °C for 5 min, at 375 °C for 5 min, at 450 °C for 15 min, and at 500 °C for 15 min. The sintered film was further treated with 0.2 M $TiCl_4$ aqueous solution at room temperature for 12 h, then washed with water and ethanol, and annealed at 450 °C for 30 min.[37] A TiO_2 electrode was dipped in the solution of **IQ21** with 3×10^{-4} M concentration in $CHCl_3$/EtOH (v/v, 7/3) for 12 h, rinsed with ethanol, and then dipped in **S2** solution (1×10^{-4} in $CHCl_3$/ethanol (7/3)) for 1−8 h. Photovoltaic measurements were performed in a sandwich-type solar cell in conjunction with an electrolyte consisting of a solution of 0.6 M dimethylpropyl-imidazolium iodide (DMPII), 0.05 M I_2, 0.1 M LiI, and 0.5−1.0 M *tert*-butylpyridine (TBP) in acetonitrile (AN). The dye-deposited TiO_2 film and a platinum-coated conducting glass were separated by a Surlyn spacer (40 μm thick) and sealed by heating the polymer frame. Photocurrent density−voltage (I−V) of sealed solar cells was measured with a metal mask of 0.12 cm^2, under illuminating the cell through the conducting glass from the anode side with a solar simulator (WXS-155S-10) at AM 1.5 illuminations (light intensities: 100 mW cm^{-2}). IPCE measurements were made on a CEP-2000 system (Bunkoh-Keiki Co. Ltd.).

Electronic impedance spectra (EIS) were recorded over a frequency range from 1×10^{-2} to 1×10^6 Hz at 25 °C, based on an impedance analyzer (Solartron Analytical, 1255B) connected with a potentiostat (Solartron Analytical, 1287) under illumination using a solar simulator (WXS-155S-10: Wacom Denso Co. Japan). The applied bias voltage and alternating current amplitude were set at the V_{oc} of DSSCs, characterized using Z-View software (Solartron Analytical).

RESULTS AND DISCUSSION

Enhancement in Molar Extinction Coefficients and Light Response. Sensitizers with high extinction coefficients show several advantages for application in DSSCs. First, such dyes allow reduced thickness of TiO_2 electrode, which results in less charge recombination sites and enables new electrolyte systems that are difficult to penetrate deeply into the mesoporous TiO_2 electrode. Second, high extinction coefficients are beneficial to the cosensitization strategy because the dye loading amount for each dye is decreased in the cosensitization process with respect to single dye sensitization due to the competitive dye adsorption. Recently, a prototype of D-A-π-A concept has become attractive, especially for

DOI: 10.1021/am508623e
ACS Appl. Mater. Interfaces 2015, 7, 5296−5304

constructing long wavelength response, high photovoltage, and photo/thermal stable organic sensitizing dyes.[12] The internal "A" in the prototype is usually composed of an electron-withdrawing chromophore, such as benzothiadiazole, benzotriazole, quinoxaline, and so on.[37−50] As shown in Figure 1, the target dye **IQ21** was designed on the basis of our previously reported D-A-π-A dye **IQ4** with a high well-performed efficiency of 9.24%.[36] The incorporation of an efficient building block CPDT in **IQ21** is aimed at enhancing its light-harvesting ability.

Figure 2a shows the absorption spectra of dye **IQ21**, along with the reference dye **IQ4** in CH_2Cl_2. Notably, **IQ21** presents

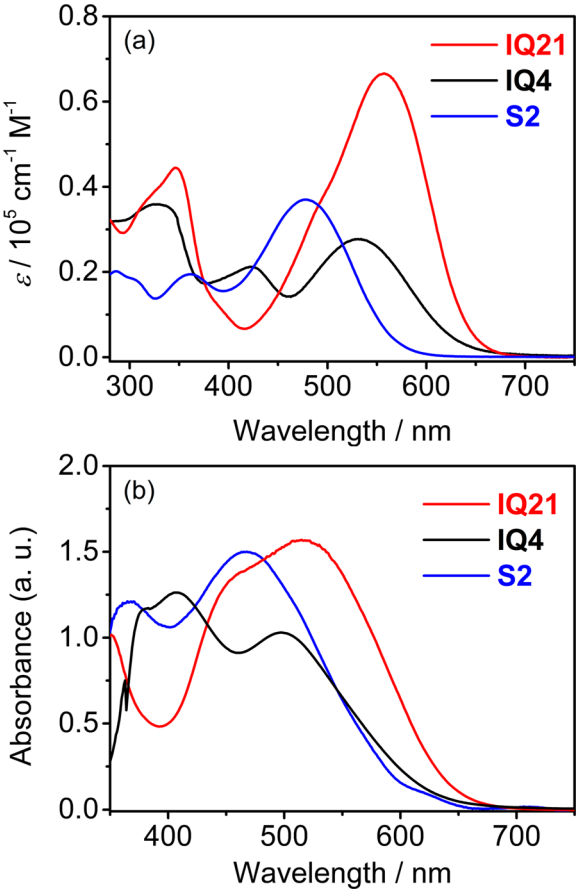

Figure 2. Absorption spectra of **IQ21**, reference dye **IQ4**, and cosensitizer **S2**: (a) in CH_2Cl_2, (b) on 4 μm TiO_2 thin films. Note: dye **S2** is screened as cosensitizer since it has a matchable molecular size with a strong absorption band in the 400−500 nm region, which is well-compensated with the optical loss of **IQ21**.

an obvious red shift in the maximum visible absorption wavelength by ~30 nm with respect to **IQ4**, which arises from the introduction of a large π-linker CPDT unit. Moreover, **IQ21** exhibits 2.6-fold higher molar extinction coefficient (6.66×10^4 M^{-1} cm^{-1}) than **IQ4** at absorption band (Table 1). As expected, replacing the thiophene unit (**IQ4**) with CPDT unit (**I21**) provides a distinct advantage for quinoxaline-based D-A-π-A type sensitizers, greatly enhancing molar extinction coefficient and light response with red shift in absorption band, which is important for obtaining high light-harvesting. In contrast, **IQ21** loses the absorption band around 420 nm, which apparently exists in **IQ4**, upon changing the π-bridge from thiophene to CPDT. Here the lower absorbance of **IQ21**

Table 1. Photophysical and Electrochemical Data of IQ21, Reference Dye IQ4, and Cosensitization Dye S2

dyes	λ_{max} in solution [nm][a]	ε [M^{-1} cm^{-1}][a]	λ_{max} on TiO_2 [nm][b]	HOMO [V][c]	E_{0-0} [V][d]	LUMO [V][d]
S2	478	32 900	465	1.02	2.06	−1.04
IQ4	531	25 700	497	0.89	1.93	−1.04
	422	21 500				
	332	35 900				
IQ21	557	66 600	518	0.84	1.92	−1.08
	346	44 800				

[a]Absorption peaks (λ_{max}) and molar extinction coefficients (ε) in the mixed solution of CH_3OH and $CHCl_3$ (v/v = 1:4). [b]Absorption peaks on TiO_2 films. [c]HOMO measured in CH_2Cl_2 with cyclic voltammograms (CV) at the scan rate of 100 mV/s. [d]E_{0-0} estimated from the absorption thresholds in absorption spectra of dyes adsorbed on TiO_2 film, LUMO estimated by subtracting E_{0-0} from the HOMO.

at ~400 nm region might decrease its light-harvesting ability in the corresponding wavelength. Therefore, the cosensitization strategy was considered for optimizing the performance of **IQ21**. Since the specific cocktail cosensitization requires suitable matches in absorption spectra and molecular structure as well as molecular size, we choose the cosensitizer **S2** (Figure 1) as a screen since it has a matchable molecular size with a strong absorption band in the 400−500 nm region (Figure 2a), which may well-compensate the corresponding optical loss of **IQ21**.

Moreover, the absorption spectra of **IQ21**, **IQ4**, and **S2** loaded TiO_2 films are shown in Figure 2b. Although the absorption band (λ_{max}) of both **IQ21** and **IQ4** are bathochromically shifted relative to those in CH_2Cl_2 solution (Table 1) due to the intermolecular interaction, the maximum absorption wavelength of **IQ21** is still 20 nm longer than that of **IQ4**. Additionally, with the same thickness of TiO_2 films, the absorbance of **IQ21**-loaded film is higher than the case of **IQ4** in the range of 430 to 700 nm. On the other hand, the absorbance of **IQ21** below 435 nm is lower than that of reference dye **IQ4**, which is in agreement with the absorption profiles in CH_2Cl_2 solution (Figure 2a). Obviously, the absorption valley of dye **IQ21** is expected to be filled by cosensitization with dye **S2** because the latter shows high absorbance at short wavelength region.

Cosensitization Effect on J_{SC} with Compensating Short Wavelength IPCE. Considering the reported reference dye **IQ4** with a well-performed photovoltaic efficiency of 9.24%,[36] we are convinced that **IQ21** with stronger light-harvesting ability should exhibit enhanced photovoltaic performance. For a clear view, a direct comparison with in-depth examination was done. The current−voltage (J−V) curves of solar cells sensitized with **IQ4** and **IQ21** measured under standard AM 1.5G simulated solar irradiation are depicted in Figure 3a, and their photovoltaic parameters are listed in Table 2. Unexpectedly, under the same condition, the DSSCs based on **IQ21** showed the photovoltaic efficiency of 9.03%, which is a little lower than that of reference dye **IQ4** (9.24%). According to the highest occupied molecular orbital (HOMO) and lowest unoccupied molecular orbital (LUMO) energy levels of both dyes in Table 1, we can rule out the mismatch possibility in energy level since the driving forces for the efficient electron injection and dye regeneration of **IQ21** and **IQ4** are thermodynamically favorable. Indeed, as expected, the J_{SC} of **IQ21** was increased by 4.3% from 17.6 (**IQ4**) to 18.3

DOI: 10.1021/am508623e
ACS Appl. Mater. Interfaces 2015, 7, 5296−5304

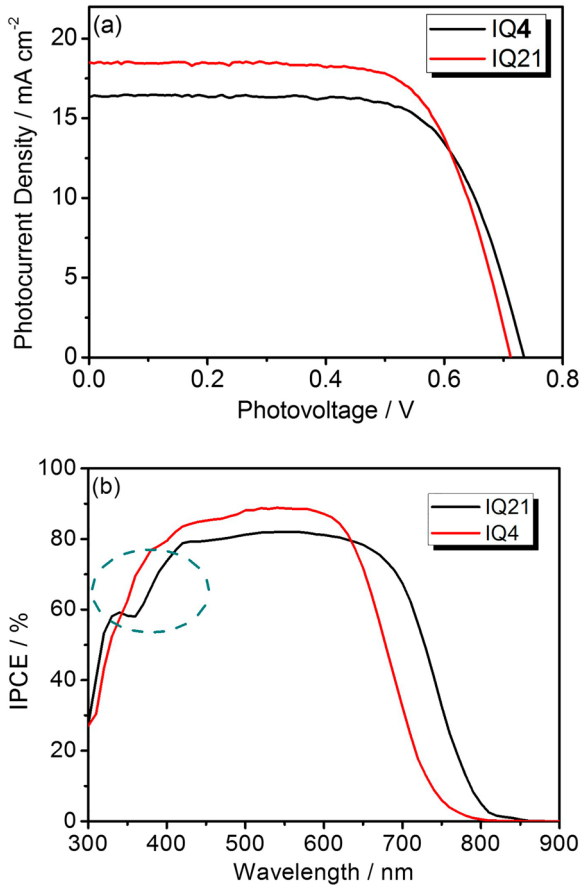

Figure 3. (a) $J-V$ curves for DSSCs based on **IQ21** and reference dye **IQ4** under AM 1.5G simulated solar light (100 mW cm^{-2}) and (b) IPCE spectra on **IQ21** and reference dye **IQ4** under dark. Note: with respect to **IQ4**, the slightly lower efficiency of **IQ21** arises from the decrease of V_{OC}, which offsets the gain in J_{SC}.

Table 2. Photovoltaic Parameters of DSSCs Based on Reference Dye IQ4, IQ21, Cosensitization of IQ21 and S2 Obtained from Four Parallel Devices under Simulated AM 1.5 Sunlight

dyes	J_{SC}, mA cm^{-2}	V_{OC}, mV	FF	η, %
IQ4	17.6 (±0.1)	740 (±5)	71.0 (±0.5)	9.2 (±0.3)
IQ21	18.3 (±0.2)	711 (±4)	69.4 (±0.3)	9.0 (±0.2)
IQ21+S2 (1 h) device D1[a]	19.8 (±0.2)	731 (±5)	72.0 (±0.3)	10.4 (±0.3)
IQ21+S2 (8 h) device D8[a]	13.2 (±0.1)	732 (±2)	70.0 (±0.5)	6.8 (±0.1)
S2+ IQ21 (1 h) device DS1[b]	18.3 (±0.3)	715 (±2)	68.6 (±0.2)	9.0 (±0.2)
S2+ IQ21 (8 h) device DS8[b]	16.0 (±0.2)	733 (±3)	71.0 (±0.5)	8.3 (±0.2)

[a]For devices D1 and D8, a TiO_2 electrode was dipped in the solution of **IQ21** with 3×10^{-4} M concentration in $CHCl_3$/EtOH (v/v, 7/3) for 12 h, rinsed with ethanol, and then dipped in cosensitizer **S2** (1×10^{-4} M) solution for 1 or 8 h. [b]For devices DS1 and DS8, a TiO_2 electrode was dipped in the solution of cosensitizer **S2** with 1×10^{-4} M concentration in $CHCl_3$/EtOH (v/v, 7/3) for 1 or 8 h, rinsed with ethanol, and then dipped in **IQ21** (1×10^{-4} M) solution for 12 h.

mA cm^{-2}. However, the V_{OC} was decreased by 3.9% from 740 (**IQ4**) to 711 mV (**IQ21**). To be exact, the slightly lower efficiency of **IQ21** is caused by the decrease of V_{OC}, which offsets the gain in J_{SC}. Comparing the IPCE spectra of both dyes, the device sensitized with **IQ21** displayed broader plateau region (420−700 nm) than that of **IQ4** (400−650 nm). Moreover, the excellent light-harvesting in long wavelength region extended to over 800 nm (Figure 3b). Indeed, because of the large conjugation bridge of CPDT, the broader plateau with long wavelength response results in an observed higher J_{SC} for **IQ21**. More carefully, the IPCE plateau of **IQ21** is a little lower than that of **IQ4** in the range of 450−640 nm, which probably results from the longer or larger size of **IQ21** than **IQ4**, making the binding geometry of **IQ21** on TiO_2 more tilted than that of **IQ4**, leading to fast charge recombination between the dye radical cation and electron in TiO_2 and resultant lower IPCE values for **IQ21**.[51,52] Therefore, the performance of **IQ21** could be further enhanced if the IPCE plateau could be improved, especially at short wavelength region.

To further optimize the performance of **IQ21**, a D-π-A dye of **S2** with two long branched chains was employed as a partner in cosensitization because its short wavelength region (Figure 2) can compensate the light harvesting of **IQ2**. Additionally, incorporation of two 2-ethylhexyl groups at the triphenylamine donor side in **S2** is expected to retard unfavorable aggregation. Generally, the loading ratio of cosensitized dyes plays an important role in the photovoltaic performance. We first optimized the dipping time of **IQ21**-TiO_2 electrode in solution of **S2** to change the loading ratio between **IQ21** and **S2**. The cosensitized TiO_2 electrode was first dipped in **IQ21** solution (300 μM in $CHCl_3$/ethanol (7/3)) for 12 h, rinsed with ethanol, then dipped in **S2** solution (100 μM in $CHCl_3$/ethanol (7/3)) for 1 or 8 h, indicated as **IQ21+S2** (1 h, denoted as device D1) and **IQ21+S2** (8 h, denoted as device D8), respectively. More cocktail details with other cosensitized dyes are shown in Table S1 in Supporting Information. Apparently, the cosensitizer of **S2** makes a preferable contribution to the photovotatic performance, probably due to the matching molecular size between **IQ21** and **S2**. Additionally, we checked the kinetic progress in the diffusion length (Figure S1 in Supporting Information) by measuring the wavelength-dependent ratio ($r_{(CE/PE)}$) of photocurrents generated by illuminating DSSCs from the counter-electrode side (CE) versus photoelectrode side (PE).[40] It is easy to find that the electrons injected by cocktail cells based on **IQ21** and **S2** can be efficiently collected in different kinds of conditions.

Upon cosensitization with **S2** for 1 h, the J_{SC} in device D1 successfully realized an increase from 18.3 (without cosensitization) to 19.8 mA cm^{-2} (Table 2). In contrast, when increasing the dipping time longer to 8 h (device D8), a negative contribution to the cosensitization was observed; that is, the J_{SC} in device D8 was decreased sharply from 18.3 (without cosensitization) to 13.2 mA cm^{-2}. Meanwhile, the V_{OC} for cosensitization devices D1 or D8 of **IQ21+S2** maintained at almost the same level (Table 2), whether dipping in **S2** for 1 or 8 h. Obviously, the dipping time is very critical to the J_{SC}, rather than V_{OC}. Figure S2 in Supporting Information shows the color change in TiO_2 adsorption electrodes with different times. Obviously, after dipping for 8 h in **S2** solution, the adsorption amounts of **IQ21** in device D8 are distinctly less than those of device D1 (dipping for 1 h), which has also been proved by the desorption measurements (Table S2 in Supporting Informa-

DOI: 10.1021/am508623e
ACS Appl. Mater. Interfaces 2015, 7, 5296−5304

tion). Upon coadsorption of **S2** for 1 and 8 h, the adsorption amount of **IQ21** was decreased from 1.6 to 1.4 and 1.1 × 10^{-7} mol cm^{-2}, respectively. That is, the adsorption of **IQ21** with **S2** is kinetically competitive. Upon increasing the dipping time, the originally adsorbed **IQ21** can be occupied by the cosensitized dye **S2**. As shown in Figure S3 in Supporting Information, it is obvious that, by changing the dipping time, 1 h dipping time in **S2** solution is the optimized condition. Accordingly, with cosensitization of **S2** (Table 2), the desorption of **IQ21** can result in a change in photocurrent output from 18.3 mA cm^{-2} (without cosensitization) to 19.8 mA cm^{-2} (D1, dipping **S2** for 1 h) to 13.2 mA cm^{-2} (D8, dipping **S2** for 8 h).

Moreover, the cosensitized photoanodes in the reverse dipping order were also studied. That is, the TiO_2 films were first immersed in cosensitized dye **S2** for 1 or 8 h and then were immersed in dye **IQ21** for 12 h (devices DS1 and DS8, Table 2), exhibiting less efficiency than their corresponding devices (devices D1 and D8). For example, compared with device D1, the efficiency of cosensitized devices in reverse order was decreased to 8.95% (V_{OC} of 715 mV, J_{SC} of 18.3 mA cm^{-2}, fill factor (FF) of 68.6, device DS1), and 8.31% (V_{OC} of 733 mV, J_{SC} of 16.0 mA cm^{-2}, FF of 71.0, device DS8) under the same condition. Actually, when carefully comparing the adsorption sequence, the effect of cosensitized dye **S2** on V_{OC} is quite different (Table 2). When considering the devices D1 and D8 in the normal dipping mode, the followed coadsorption of **S2** with smaller molecular volume can guarantee the dye coverage to a great extent whether or not 1 or 8 h. That is why the V_{OC} for cosensitization devices D1 or D8 of **IQ21**+**S2** maintained at almost the same level. However, when changing into the reverse dipping order, the molecular cosensitized dye **S2** only enables the dye coverage more sufficient in DS8, which may block the recombination between the injected electrons and the redox species, thus presenting a relatively higher V_{OC}.

Considering the outstanding performance of DSSCs based on **IQ21**+**S2** (1 h, device D1), the IPCE spectra were subsequently measured to further illustrate the real effect on the coabsorption of **S2**. The cell sensitized with only **IQ21** had a broad IPCE spectrum extending across the whole visible range into 850 nm and displayed the highest IPCE value (82%) in the wavelength range from 450 to 650 nm (Figure 4a). Notably, the decrease of the IPCE to ∼55% in the range of 350−450 nm left a problem to be solved in this part. Upon coabsorption with **S2** (device D1), there was nearly no influence on the onset of IPCE with respect to single **IQ21** (Figure 4a). However, the defect at ∼400 nm of IPCE spectra was compensated, which was in agreement with their normalized absorption spectra (Figure 2a). Moreover, the competitive light absorption by I_3^- in the electrolyte affects the light-harvesting efficiency of dyes in the wavelength range from 350 to 400 nm. Here the cosensitization with **S2** can recover the IPCE loss caused by I_3^- (Figure 4a). Actually, **S2** has two absorption peaks, at 368 and 465 nm (Figure 2a), which can exactly compensate light absorption in the region for enhancing light harvesting. Additionally, the IPCE value based on cosensitization was also slightly higher than that based on only **IQ21**. Hence the J_{SC} value in cosensitization device D1 (Figure 4b) was further increased to 19.8 mA cm^{-2} with respect to that sensitized with **IQ21**-based cells (18.3 mA cm^{-2}), which is in good accordance with their IPCE spectra. Furthermore, a V_{OC} enhancement of 20 mV was achieved by the coabsorption of **S2** with **IQ21**. As listed in Table 2, the measured V_{OC} (731 mV) in cosensitization device D1 was fairly close to that of **IQ4**

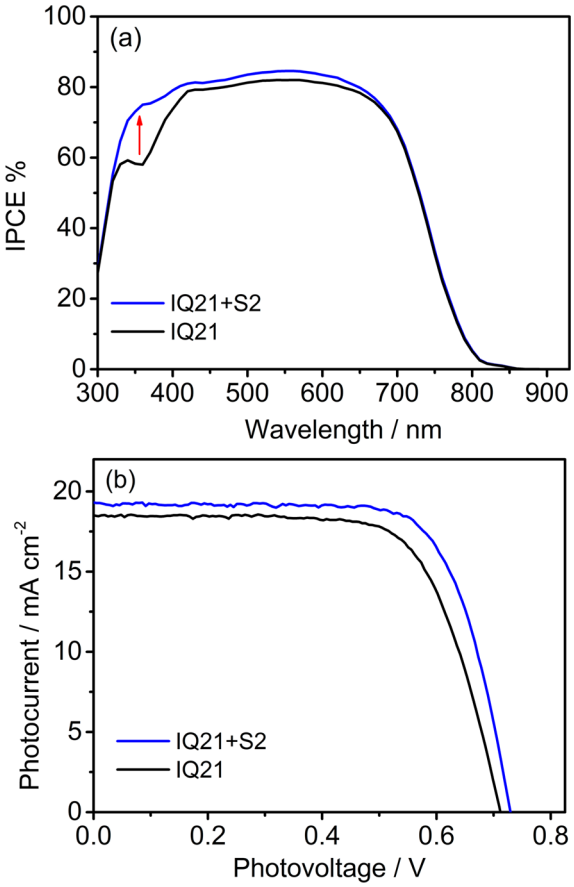

Figure 4. DSSCs based on dye **IQ21**, cosensitization of **IQ21** and **S2** (device D1, dipping **S2** for 1 h): (a) *J*−*V* curves under AM 1.5G simulated solar light (100 mW cm^{-2}), (b) IPCE spectra under dark. Note: the cocktail cosensitization with **S2** can not only increase the photocurrent with compensating the short wavelength light response but also get an improvement in photovoltage.

(740 mV). Taken together, we provide the cocktail cosensitization with **S2** (device D1, Table 2) to simultaneously improve both J_{SC} and V_{OC}, thus resulting in a very promising photovoltaic efficiency of 10.41% (J_{SC} = 19.8 mA cm^{-2}, V_{OC} = 731 mV, FF = 0.72). Furthermore, the overall efficiency remained at 98% of the initial value after 1000 h of visible-light soaking, which demonstrates the high stability of DSSCs based on **IQ21**+**S2** (device D1, Figure 5).

Cosensitization Effect on V_{OC} via Repressing the Charge Recombination Rate. Upon cocktail cosensitization with **S2**, the V_{OC} for fabricated devices D1 or D8 can be enhanced by 20 mV, even maintaining at almost the same level (Table 2) whether dipping for 1 or 8 h. Generally, EIS measurement is the most immediate way to check the origin in the variation of V_{OC}. We also scrutinized the conduction band position of TiO_2 and the charge recombination rate in DSSCs based on these three reported sensitizers. Actually, the V_{OC} is originated from the potential difference between the quasi-Fermi level of TiO_2 (E_{Fn}) and the redox species (E_{red}) in the electrolyte.[53,54] Since the redox potential is kept constant due to the same redox couples used in the experiment, the V_{OC} value is determined by the position of TiO_2 conduction band and the electron density in the semiconductor.[55−57] Here we exploited the fitted capacitive (C_μ) response of cells under a series bias potential to study the impact on the position of TiO_2 conduction band. For DSSCs based on **IQ21**, cosensitization of

DOI: 10.1021/am508623e
ACS Appl. Mater. Interfaces 2015, 7, 5296−5304

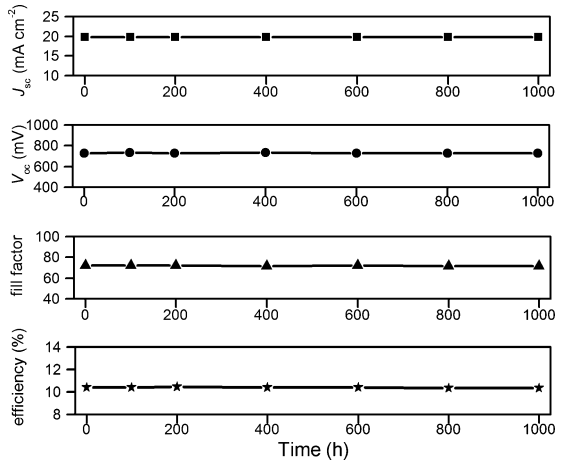

Figure 5. Variation of photovoltaic parameters with aging time for DSSC device based on **IQ21**+**S2** (dipping **S2** for 1 h, device 1) under visible-light soaking.

IQ21 with **S2** (dipping **S2** for 1 h, device D1) and reference dye **IQ4**, the logarithm of C_μ was increased linearly with the given bias potential, and all the curves exhibited the almost identical slope (Figure 6a). At fixed potential, the same C_μ values for these DSSCs indicated that the conduction band position of TiO_2 was not essentially influenced.

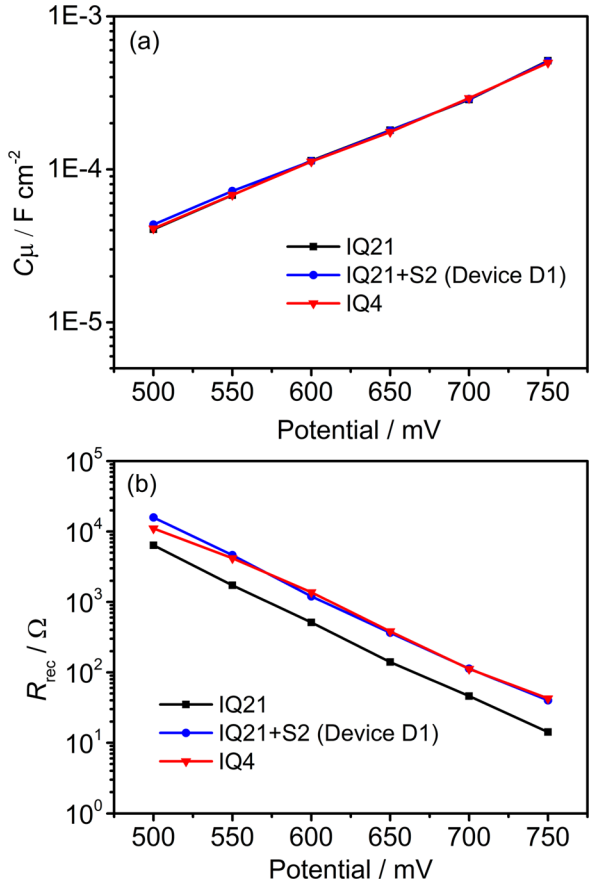

Figure 6. Plot curves under a series potential bias of DSSCs based on reference dye **IQ4**, **IQ21**, and cosensitization of **IQ21** and **S2** with dipping **S2** for 1 h (devices D1): (a) cell capacitance (C_μ), and (b) recombination resistance (R_{rec}).

As shown in Figure 6b, the fitted recombination resistance (R_{rec}) of cosensitization-based DSSCs was always larger than that of **IQ21**-based DSSCs. Meanwhile, the curves of **IQ21**+**S2** (D1) and **IQ4**-based DSSCs were overlapped very well, in good agreement with their similar V_{OC} values (Table 2). Here the cosensitization increase in V_{OC} for device D1 should be predominantly arisen from the repression of charge recombination, resulting in the higher electron density in TiO_2 conduction band cocktail than that of **IQ21** only. Obviously, the introduction of the coabsorbent with bulk chains such as **S2** can distinctly compensate the inherent drawbacks of **IQ21**, not only enhancing the response intensity of IPCE, making up the absorption defects around low wavelength region of IPCE, but also repressing the charge recombination rate to some extent.[58]

Theoretical Approach. Time-dependent density functional theory calculations performed with Gaussian 09 program package at the B3LYP/6-31G* (LANL2DZ for Ti atom) level were employed in further exploring the dependence of charge recombination on the molecular geometries and orbitals.[59] The cosensitizer of **S2** contains two bulky 2-ethylhexyl groups at the triphenylamine donor side. It is well-known that the effective surface blocking is vital for long electron lifetime.[60−62] As simulated, the vertical lengths of **S2** and **IQ21** were 20.3 and 20.6−22.8 Å (Figure 7), respectively.

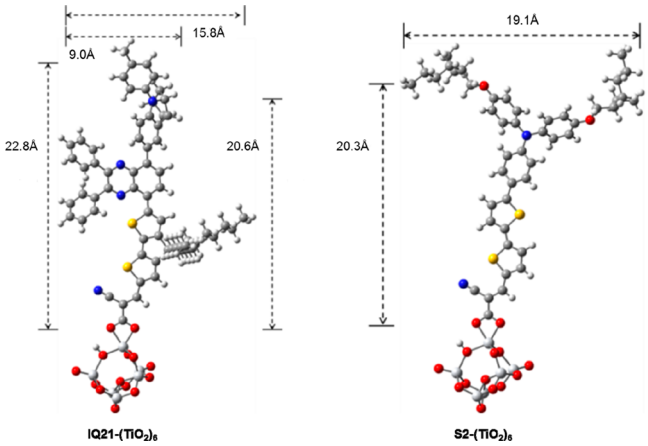

Figure 7. Optimized molecular structures of **IQ21** and cosensitizer **S2** derived from density functional theory calculations (B3LYP/6-31G*).

That is, the molecular size of **S2** and **IQ21** matches very well. Moreover, **S2** and **IQ21** can be located well-above the TiO_2 surface for retarding the rate of interfacial back electron transfer from the conduction band of the **TiO_2** film to the electrolyte I_3^- ions, thus resulting in attainment of higher photovoltage. Indeed, **S2** has potential tendency to overcome the barrier of alkoxy chain and anchor on the TiO_2 film due to the well-matched π-bridge length. Besides the alkoxy-chains, the cosensitization of **S2** with proper conjugation bridge can guarantee further forming a compact sensitized layer for preventing I_3^- from approaching to TiO_2 film.

CONCLUSIONS

Novel D-A-π-A featured sensitizer **IQ21**, consisting of indoline unit as electron donor, cyanoacetic acid as acceptor/anchor, quinoxaline unit as the auxiliary acceptor, and CPDT unit as the π-conjugation has been specifically developed for highly efficient DSSC. Utilizing **IQ4** as the reference sensitizer, we demonstrate a clear motivation to investigate the general

DOI: 10.1021/am508623e
ACS Appl. Mater. Interfaces 2015, 7, 5296−5304

influence of different π-spacer in these D-A-π-A featured organic sensitizers on their absorption, energy levels, and photovoltaic performances. As found, the replacement of thiophene unit by CPDT unit shows a red shift in absorption band, extreme enhancement in maximum molar extinction coefficient, but little influence in energy levels. We have established a promising cocktail cosensitization system of **IQ21** and **S2**, exhibiting an optimized high photovoltaic efficiency of 10.41% (J_{SC} = 19.8 mA cm^{-2}, V_{OC} = 731 mV, FF = 0.72). The coadsorbent **S2** with two long branch chains not only effectively shields the back electron transfer from the TiO_2 to I_3^- ions but also enhances the light-harvesting ability in the short wavelength regions. Our work well illustrates how to rationally increase molecular extinction coefficients and step by step optimize photovoltaic efficiency with cocktail cosensitization. Further exploration is focused on cosensitized dyes with matchable molecular sizes, shapes, and orientations.

■ ASSOCIATED CONTENT

Supporting Information

Synthetic route of **IQ21**, the color image of TiO_2 electrodes based on **IQ21**, **IQ21+S2** (8 h, device D8), and **IQ21+S2** (1 h, device D1), kinetics investigations, parameters versus dipping times, photovoltaic parameters of DSSCs, and ^{1}H, ^{13}C NMR and HRMS of **IQ21**. This material is available free of charge via the Internet at http://pubs.acs.org.

■ AUTHOR INFORMATION

Corresponding Author

*Fax: (+86) 21-6425-2758. E-mail: whzhu@ecust.edu.cn.

Author Contributions

§K.P. and Y.Z.W. contributed equally.

Notes

The authors declare no competing financial interest.

■ ACKNOWLEDGMENTS

This work was supported by NSFC for Creative Research Groups (21421004) and Distinguished Young Scholars (21325625), NSFC/China, the Oriental Scholarship, National Major Scientific Technological Special Project (2012YQ15008709), and the Fundamental Research Funds for the Central Universities (WJ1416005).

■ REFERENCES

(1) O'Regan, B.; Grätzel, M. A Low-Cost, High-Efficiency Solar Cell Based on Dye-Sensitized Colloidal TiO_2 Films. *Nature* **1991**, *353*, 737−740.

(2) Ahmad, S.; Nazeeruddin, M. K.; Bisquert, J. Hybrid Organic−Inorganic Photovoltaics. *ChemPhysChem* **2014**, *15*, 987−989.

(3) Hagfeldt, A.; Boschloo, G.; Sun, L.; Kloo, L.; Pettersson, H. Dye-Sensitized Solar Cells. *Chem. Rev.* **2010**, *110*, 6595−6663.

(4) Mishra, A.; Fischer, M. K. R.; Bäuerle, P. Metal-Free Organic Dyes for Dye-Sensitized Solar Cells: From Structure: Property Relationships to Design Rules. *Angew. Chem., Int. Ed.* **2009**, *48*, 2474−2499.

(5) Qu, S. Y.; Hua, J. L.; Tian, H. New D-π-A Dyes for Efficient Dye-Sensitized Solar Cells. *Sci. China Chem.* **2012**, *55*, 677−697.

(6) Li, C.; Wonneberger, H. Perylene Imides for Organic Photovoltaics: Yesterday, Today, and Tomorrow. *Adv. Mater.* **2012**, *24*, 613−636.

(7) Liang, M.; Chen, J. Arylamine Organic Dyes for Dye-Sensitized Solar Cells. *Chem. Soc. Rev.* **2013**, *42*, 3453−3488.

(8) Chou, C. C.; Hu, F. C.; Yeh, H. H.; Wu, H. P.; Chi, Y.; Clifford, J. N.; Palomares, E.; Liu, S. H.; Chou, P. T.; Lee, G. H. Highly Efficient Dye-Sensitized Solar Cells Based on Panchromatic Ruthenium Sensitizers with Quinolinylbipyridine Anchors. *Angew. Chem., Int. Ed.* **2014**, *53*, 178−183.

(9) Pang, A.; Xia, L.; Luo, H.; Li, Y.; Wei, M. Highly Efficient Indoline Dyes Co-sensitized Solar Cells Composed of Titania Nanorods. *Electrochim. Acta* **2013**, *94*, 92−97.

(10) Yen, Y. S.; Chou, H. H.; Chen, Y. C.; Hsu, C. Y.; Lin, J. T. Recent Developments in Molecule-Based Organic Materials for Dye-Sensitized Solar Cells. *J. Mater. Chem.* **2012**, *22*, 8734−8747.

(11) Wu, Y. Z.; Zhu, W. H. Organic Sensitizers from D-π-A to D-A-π-A: Effect of the Internal Electron-Withdrawing Units on Molecular Absorption, Energy Levels and Photovoltaic Performances. *Chem. Soc. Rev.* **2013**, *42*, 2039−2058.

(12) Peter, L. M. The Grätzel Cell: Where Next? *J. Phys. Chem. Lett.* **2011**, *2*, 1861−1867.

(13) Ahmad, S.; Guillén, E.; Kavan, L.; Grätzel, M.; Nazeeruddin, M. K. Metal Free Sensitizer and Catalyst for Dye Sensitized Solar Cells. *Energy Environ. Sci.* **2013**, *6*, 3439−3466.

(14) Li, Q.; Jiang, Z.; Qin, J.; Li, Z. Heterocyclic-Functionalized Organic Dyes for Dye-Sensitized Solar Cells: Tuning Solar Cell Performance by Structural Modification. *Aust. J. Chem.* **2012**, *65*, 1203−1212.

(15) Zeng, W.; Cao, Y.; Bai, Y.; Wang, Y.; Shi, Y.; Zhang, M.; Wang, F.; Pan, C.; Wang, P. Efficient Dye-Sensitized Solar Cells with an Organic Photosensitizer Featuring Orderly Conjugated Ethylenedioxythiophene and Dithienosilole Blocks. *Chem. Mater.* **2010**, *22*, 1915−1925.

(16) Zhang, M.; Wang, Y.; Xu, M.; Ma, W.; Li, R.; Wang, P. Design of High-Efficiency Organic Dyes for Titania Solar Cells Based on the Chromophoric Core of Cyclopentadithiophene-Benzothiadiazole. *Energy Environ. Sci.* **2013**, *6*, 2944−2949.

(17) Luo, J.; Xu, M.; Li, R.; Huang, K.; Jiang, C.; Qi, Q.; Zeng, W.; Zhang, J.; Chi, C.; Wang, W.; Wu, J. *N*-Annulated Perylene as an Efficient Electron Donor for Porphyrin-Based Dyes: Enhanced Light-Harvesting Ability and High-Efficiency Co(II/III)-Based Dye-Sensitized Solar Cells. *J. Am. Chem. Soc.* **2014**, *136*, 265−272.

(18) Yang, J.; Ganesan, P.; Teuscher, J.; Moehl, T.; Kim, Y. J.; Yi, C.; Comte, P.; Pei, K.; Holcombe, T. W.; Nazeeruddin, M. K.; Hua, J.; Zakeeruddin, S. M.; Tian, H.; Grätzel, M. Influence of the Donor Size in D-π-A Organic Dyes for Dye-Sensitized Solar Cells. *J. Am. Chem. Soc.* **2014**, *136*, 5722−5730.

(19) Li, Y.; Wang, H.; Feng, Q.; Zhou, G.; Wang, Z. S. Gold Nanoparticles Inlaid TiO_2 Photoanodes: a Superior Candidate for High-Efficiency Dye-Sensitized Solar Cells. *Energy Environ. Sci.* **2013**, *6*, 2156−2165.

(20) Zhang, S.; Islam, A.; Yang, X.; Qin, C.; Zhang, K.; Numata, Y.; Chen, H.; Han, L. Improvement of Spectral Response by Co-sensitizers for High Efficiency Dye-Sensitized Solar Cells. *J. Mater. Chem. A* **2013**, *1*, 4812−4819.

(21) Mathew, S.; Yella, A.; Gao, P.; Humphry-Baker, R.; Curchod, B. F. E.; Ashari-Astani, N.; Tavernelli, I.; Rothlisberger, U.; Nazeeruddin, M. K.; Grätzel, M. Dye-sensitized Solar Cells with 13% Efficiency Achieved through the Molecular Engineering of Porphyrin Sensitizers. *Nat. Chem.* **2014**, *6*, 242−247.

(22) Yum, J.-H.; Baranoff, E.; Wenger, S.; Nazeeruddin, M. K.; Grätzel, M. Panchromatic Engineering for Dye-Sensitized Solar Cells. *Energy Environ. Sci.* **2011**, *4*, 842−857.

(23) Yum, J.-H.; Hardin, B. E.; Hoke, E. T.; Baranoff, E.; Zakeeruddin, S. M.; Nazeeruddin, M. K.; Torres, T.; McGehee, M. D.; Grätzel, M. Incorporating Multiple Energy Relay Dyes in Liquid DyeSensitized Solar Cells. *ChemPhysChem* **2011**, *12*, 657−661.

(24) Hardin, B. E.; Sellinger, A.; Moehl, T.; Humphry-Baker, R.; Moser, J.-E.; Wang, P.; Zakeeruddin, S. M.; Grätzel, M.; McGehee, M. D. Energy and Hole Transfer between Dyes Attached to Titania in Co-sensitized Dye-Sensitized Solar Cells. *J. Am. Chem. Soc.* **2011**, *133*, 10662−10667.

(25) Hardin, B. E.; Yum, J.-H.; Hoke, E. T.; Jun, Y. C.; Péchy, P.; Torres, T.; Brongersma, M. L.; Nazeeruddin, M. K.; Grätzel, M.; McGehee, M. D. High Excitation Transfer Efficiency from Energy

DOI: 10.1021/am508623e
ACS Appl. Mater. Interfaces 2015, 7, 5296−5304

Relay Dyes in Dye-Sensitized Solar Cells. *Nano Lett.* **2010**, *10*, 3077−3083.
(26) Hardin, B. E.; Hoke, E. T.; Armstrong, P. B.; Yum, J.-H.; Comte, P.; Torres, T.; Frechet, J. M. J.; Nazeeruddin, M. K.; Grätzel, M.; McGehee, M. D. Increased Light Harvesting in Dye-Sensitized Solar Cells. *Nat. Photonics* **2009**, *3*, 406−411.
(27) Han, L. Y.; Islam, A.; Chen, H.; Malapaka, C.; Chiranjeevi, B.; Zhang, S. F.; Yang, X. D.; Yanagida, M. High-Efficiency Dye-Sensitized Solar Cell with a Novel Co-adsorbent. *Energy Environ. Sci.* **2012**, *5*, 6057−6060.
(28) Li, H.; Wu, Y. Z.; Geng, Z. Y.; Liu, J. C.; Xu, D. D.; Zhu, W. H. Co-sensitization of Benzoxadiazole Based D-A-π-A Featured Sensitizers: Compensating Light-Harvesting and Retarding Charge Recombination. *J. Mater. Chem. A* **2014**, *2*, 14649−14657.
(29) Yella, A.; Lee, H.-W.; Tsao, H. N.; Yi, C.; Chandiran, A. K.; Nazeeruddin, M. K.; Diau, E. W.-G.; Yeh, C.-Y.; Zakeeruddin, S. M.; Grätzel, M. Porphyrin-Sensitized Solar Cells with Cobalt (II/III)−Based Redox Electrolyte Exceed 12% Efficiency. *Science* **2011**, *334*, 629−634.
(30) Li, L.; Diau, E. W. Porphyrin-Sensitized Solar Cells. *Chem. Soc. Rev.* **2013**, *42*, 291−304.
(31) Hiqashino, T.; Imahori, H. Porphyrins as Excellent Dyes for Dye-Sensitized Solar Cells: Recent Developments and Insights. *Dalton Trans.* **2015**, *44*, 448−463.
(32) Ying, L.; Hsu, B. B. Y.; Zhan, H.; Welch, G. C.; Zalar, P.; Perez, L. A.; Kramer, E. J.; Nguyen, T. Q.; Heeger, A. J.; Wong, W. Y.; Bazan, G. C. Regioregular Pyridal[2,1,3]thiadiazole π-Conjugated Copolymers. *J. Am. Chem. Soc.* **2011**, *133*, 18538−18541.
(33) Horie, M.; Kettle, J.; Yu, C.-Y.; Majewski, L. A.; Chang, S.-W.; Kirkpatrick, J.; Tuladhar, S. M.; Nelson, J.; Saunders, B. R.; Turner, M. L. Cyclopentadithiophene-Benzothiadiazole Oligomers and Polymers; Synthesis, Characterisation, Field-Effect Transistor and Photovoltaic Characteristics. *J. Mater. Chem.* **2012**, *22*, 381−389.
(34) Zhang, M.; Zhang, J.; Fan, Y.; Yang, L.; Wang, Y.; Li, R.; Wang, P. Judicious Selection of a Pinhole Defect Filler to Generally Enhance the Performance of Organic Dye-Sensitized Solar Cells. *Energy Environ. Sci.* **2013**, *6*, 2939−2943.
(35) Kang, X. W.; Zhang, J. X.; Rojas, A. J.; O'Neil, D.; Szymanski, P.; Marder, S. R.; El-Sayed, M. A. Deposition of Loosely Bound Organic D-A-π-A′ Dyes on Sensitized TiO_2 Film: a Possible Strategy to Suppress Charge Recombination and Enhance Power Conversion Efficiency in Dye-Sensitized Solar Cells. *J. Mater. Chem. A* **2014**, *2*, 11229−11234.
(36) Pei, K.; Wu, Y. Z.; Islam, A.; Zhang, Q.; Han, L. Y.; Tian, H.; Zhu, W. H. Constructing High-Efficiency D-A-π-A-Featured Solar Cell Sensitizers: a Promising Building Block of 2,3-Diphenylquinoxaline for Antiaggregation and Photostability. *ACS Appl. Mater. Interfaces* **2013**, *5*, 4986−4995.
(37) Pei, K.; Wu, Y. Z.; Wu, W. J.; Zhang, Q.; Chen, B. Q.; Tian, H.; Zhu, W. H. Constructing Organic D-A-π-A-Featured Sensitizers with a Quinoxa-line Unit. *Chem.—Eur. J.* **2012**, *18*, 8190−8200.
(38) Wu, Y. Z.; Marszalek, M.; Zakeeruddin, S. M.; Zhang, Q.; Tian, H.; Grätzel, M.; Zhu, W. H. High-Conversion-Efficiency Organic Dye-Sensitized Solar Cells: Molecular Engineering on D-A-π-A Featured Organic Indoline Dyes. *Energy Environ. Sci.* **2012**, *5*, 8261−8272.
(39) Chai, Q. P.; Qin, W.; Zhu, S. Q.; Zhang, Q.; Zhu, W. H. Influence of Donor Configurations on Photophysical, Electrochemical and Photovoltaic Performances in D-π-A Organic Sensitizers. *ACS Sustainable Chem. Eng.* **2014**, *2*, 239−247.
(40) Pei, K.; Wu, Y. Z.; Islam, A.; Zhu, S. Q.; Han, L. Y.; Geng, Z. Y.; Zhu, W. H. Dye-Sensitized Solar Cells Based on Quinoxaline Dyes: Effect of π-Linker on Absorption, Energy Levels, and Photovoltaic Performances. *J. Phys. Chem. C* **2014**, *118*, 16552−16561.
(41) Li, S. R.; Lee, C. P.; Kuo, H. T.; Ho, K. C.; Sun, S. S. High-Performance Dipolar Organic Dyes with an Electron-Deficient Diphenylquinoxaline Moiety in the π-Conjugation Framework for Dye-Sensitized Solar Cells. *Chem.—Eur. J.* **2012**, *18*, 12085−12095.
(42) Shi, J.; Chen, J. N.; Chai, Z. F.; Wang, H.; Tang, R. L.; Fan, K.; Wu, M.; Han, H. W.; Qin, J. G.; Peng, T. Y.; Li, Q. Q.; Li, Z. High Performance Organic Sensitizers Based on 11,12-bis(hexyloxy) Dibenzo [*a*,*c*]phenazine for Dye-Sensitized Solar Cells. *J. Mater. Chem.* **2012**, *22*, 18830−18838.
(43) Lu, X. F.; Feng, Q. Y.; Lan, T.; Zhou, G.; Wang, Z. S. Molecular Engineering of Quinoxaline-Based Organic Sensitizers for Highly Efficient and Stable Dye-Sensitized Solar Cells. *Chem. Mater.* **2012**, *24*, 3179−3187.
(44) Li, S. R.; Lee, C. P.; Yang, P. F.; Liao, C. W.; Lee, M. M.; Su, W. L.; Li, C. T.; Lin, H. W.; Ho, K. C.; Sun, S. S. Structure−Performance Correlations of Organic Dyes with an Electron-Deficient Diphenylquinoxaline Moiety for Dye-Sensitized Solar Cells. *Chem.—Eur. J.* **2014**, *20*, 10052−10064.
(45) Li, H. R.; Koh, T. M.; Hagfeldt, A.; Grätzel, M.; Mhaisalkar, S. G.; Grimsdale, A. C. New Donor−π−Acceptor Sensitizers Containing 5*H*-[1,2,5]thiadiazolo[3,4-*f*]isoindole-5,7(6*H*)-dione and 6*H*-pyrrolo-[3,4-*g*]quinoxaline-6,8(7*H*)-dione Units. *Chem. Commun.* **2013**, *49*, 2409−2411.
(46) Feng, Q. Y.; Zhang, W. Y.; Zhou, G.; Wang, Z. S. Enhanced Performance of Quasi-Solid-State Dye-Sensitized Solar Cells by Branching the Linear Substituent in Sensitizers Based on Thieno [3,4-*c*]pyrrole-4,6-dione. *Chem.—Asian J.* **2013**, *8*, 168−177.
(47) Li, S. R.; Lee, C. P.; Liao, C. W.; Su, W. L.; Li, C. T.; Ho, K. C.; Sun, S. S. Structural Engineering of Dipolar Organic Dyes with an Electron-Deficient Diphenylquinoxaline Moiety for Efficient Dye-Sensitized Solar Cells. *Tetrahedron* **2014**, *70*, 6276−6284.
(48) Feng, Q. Y.; Jia, X. W.; Zhou, G.; Wang, Z. S. Embedding an Electron Donor or Acceptor into Naphtho[2,1-*b*:3,4-*b*′]dithiophene Based Organic Sensitizers for Dye-Sensitized Solar Cells. *Chem. Commun.* **2013**, *49*, 7445−7447.
(49) Lin, Y. Z.; Huang, C. H.; Chang, Y. J.; Yeh, C. W.; Chin, T. M.; Chi, K. M.; Chou, P. T.; Watanabe, M.; Chow, T. J. Anthracene Based Organic Dipolar Compounds for Sensitized Solar Cells. *Tetrahedron* **2014**, *70*, 262−269.
(50) Haid, S.; Marszalek, M.; Mishra, A.; Wielopolski, M.; Teuscher, J.; Moser, J.; Humphry-Baker, R.; Zakeeruddin, S. M.; Grätzel, M.; Bäuerle, P. Significant Improvement of Dye-Sensitized Solar Cell Performance by Small Structural Modification in π-Conjugated Donor-Acceptor Dyes. *Adv. Funct. Mater.* **2012**, *22*, 1291−1302.
(51) Imahori, H.; Kang, S.; Hayashi, H.; Haruta, M.; Kurata, H.; Isoda, S.; Canton, S. E.; Infahsaeng, Y.; Kathiravan, A.; Pascher, T.; Chábera, P.; Yartsev, A. P.; Sundström, V. Photoinduced Charge Carrier Dynamics of Zn−Porphyrin−TiO_2 Electrodes: The Key Role of Charge Recombination for Solar Cell Performance. *J. Phys. Chem. A* **2011**, *115*, 3679−3690.
(52) Ye, S.; Kathiravan, A.; Hayashi, H.; Tong, Y.; Infahsaeng, Y.; Chabera, P.; Pascher, T.; Yartsev, A. P.; Isoda, S.; Imahori, H.; Sundström, V. Role of Adsorption Structures of Zn-Porphyrin on TiO_2 in Dye-Sensitized Solar Cells Studied by Sum Frequency Generation Vibrational Spectroscopy and Ultrafast Spectroscopy. *J. Phys. Chem. C* **2013**, *117*, 6066−6080.
(53) Usami, A.; Seki, S.; Mita, Y.; Kobayashi, H.; Miyashiro, H.; Terada, N. Temperature Dependence of Open-Circuit Voltage in Dye-Sensitized Solar Cells. *Sol. Energy Mater. Sol. Cells* **2009**, *93*, 840−842.
(54) Lu, M.; Liang, M.; Han, H.; Sun, Z.; Xue, S. Organic Dyes Incorporating Bis-hexapropyltruxeneamino Moiety for Efficient Dye-Sensitized Solar Cells. *J. Phys. Chem. C* **2011**, *115*, 274−281.
(55) Fabregat-Santiago, F.; Garcia-Belmonte, G.; Mora-Seró, I.; Bisquert, J. Characterization of Nanostructured Hybrid and Organic Solar Cells by Impedance Spectroscopy. *J. Phys. Chem. Chem. Phys.* **2011**, *13*, 9083−9118.
(56) Stergiopoulos, T.; Falaras, P. Minimizing Energy Losses in Dye-Sensitized Solar Cells Using Coordination Compounds as Alternative Redox Mediators Coupled with Appropriate Organic Dyes. *Adv. Energy Mater.* **2012**, *2*, 616−627.
(57) Li, L. L.; Chang, Y. C.; Wu, H. P.; Diau, E. W. G. Characterisation of Electron Transport and Charge Recombination Using Temporally Resolved and Frequency-Domain Techniques for Dye-Sensitised Solar Cells. *Int. Rev. Phys. Chem.* **2012**, *31*, 420−467.

DOI: 10.1021/am508623e
ACS Appl. Mater. Interfaces 2015, 7, 5296−5304

(58) Giazitzidis, P.; Argyrakis, P.; Bisquert, J.; Vikhrenko, V. S. Charge Separation in Organic Photovoltaic Cells. *Org. Electron.* **2014**, *15*, 1043−1049.
(59) Frisch, M. J.; Trucks, G. W.; Schlegel, H. B.; Scuseria, G. E.; Robb, M. A.; Cheeseman, J. R.; Scalmani, G.; Barone, V.; Mennucci, B.; Petersson, G. A.; Nakatsuji, H.; Caricato, M.; Li, X.; Hratchian, H. P.; Izmaylov, A. F.; Bloino, J.; Zheng, G.; Sonnenberg, J. L.; Hada, M.; Ehara, M.; Toyota, K.; Fukuda, R.; Hasegawa, J.; Ishida, M.; Nakajima, T.; Honda, Y.; Kitao, O.; Nakai, H.; Vreven, T.; Montgomery, J. A.; Peralta, J. E.; Ogliaro, F.; Bearpark, M.; Heyd, J. J.; Brothers, E.; Kudin, K. N.; Staroverov, V. N.; Kobayashi, R.; Normand, J.; Raghavachari, K.; Rendell, A.; Burant, J. C.; Iyengar, S. S.; Tomasi, J.; Cossi, M.; Rega, N.; Millam, J. M.; Klene, M.; Knox, J. E.; Cross, J. B.; Bakken, V.; Adamo, C.; Jaramillo, J.; Gomperts, R.; Stratmann, R. E.; Yazyev, O.; Austin, A. J.; Cammi, R.; Pomelli, C.; Ochterski, J. W.; Martin, R. L.; Morokuma, K.; Zakrzewski, V. G.; Voth, G. A.; Salvador, P.;Dannenberg, J. J.; Dapprich, S.; Daniels, A. D.; Farkas, O.; Foresman, J. B.; Ortiz, J. V.; Cioslowski, J.; Fox, D. J. *Gaussian 09,* Revision A.02; Gaussian, Inc.: Wallingford, CT, 2009.
(60) Privalov, T.; Boschloo, G.; Hagfeldt, A.; Svensson, P. H.; Kloo, L. A Study of the Interactions between I^-/I_3^- Redox Mediators and Organometallic Sensitizing Dyes in Solar Cells. *J. Phys. Chem. C* **2009**, *113*, 783−790.
(61) Planells, M.; Pellejá, L.; Clifford, J. N.; Pastore, M.; Angelis, F. D.; López, N.; Marder, S. R.; Palomares, E. Energy Levels, Charge Injection, Charge Recombination and Dye Regeneration Dynamics for Donor-Acceptor π-Conjugated Organic Dyes in Mesoscopic TiO_2 Sensitized Solar Cells. *Energy Environ. Sci.* **2011**, *4*, 1820−1829.
(62) Tuikka, M.; Hirva, P.; Rissanen, K.; Korppi-Tommola, J.; Haukka, M. Halogen Bonding-a Key Step in Charge Recombination of the Dye-Sensitized Solar Cell. *Chem. Commun.* **2011**, *47*, 4499−4501.

DOI: 10.1021/am508623e
ACS Appl. Mater. Interfaces 2015, 7, 5296−5304